Wetting of Superfluid ^{4}He by Liquid ^{3}He

H. Alles, J. P. Ruutu, A. V. Babkin, and P. J. Hakonen
Low Temperature Laboratory, Helsinki University of Technology, 02150 Espoo, Finland
(Received 9 March 1994)

We have investigated optically the spreading of ^{3}He on top of the ^{4}He-rich solution in phase-separated helium-mixture films, 20–50 μm thick. In equilibrium, the ^{3}He layer wets the ^{4}He-rich phase completely, but nearly circular or stripelike pools of ^{3}He-rich phase are stabilized instead when ^{4}He atoms are condensed to the liquid sample at the rate 10^{15}–5×10^{15} atoms/cm^2 s. For the contact angle we obtain about 10 mrad, which suggests a fractional change of the ^{3}He surface tension by a factor of 10^{-5} from the equilibrium value.

PACS numbers: 67.60.Fp

Superfluid ^{4}He was considered, for a long time, a perfect wetting agent of solid surfaces at low temperature. Recently, however, anomalous wetting phenomena have been observed: Below $T_w = 1.95$ K superfluid ^{4}He fails to wet cesium surfaces [1,2]. This finding has given rise to enhanced interest in wetting phenomena at low temperatures [3]. Reentrant wetting behavior has been found in ^{3}He/^{4}He mixtures [4,5] while pure liquid ^{3}He is expected to wet Cs on theoretical grounds [6].

In this Letter we report that, under certain nonequilibrium conditions, liquid ^{3}He does not wet superfluid ^{4}He. We have discovered, using interferometric techniques developed in our laboratory [7], that in an experimental cell containing a thin layer of phase-separated ^{3}He/^{4}He mixture the upper ^{3}He-rich phase is not able to wet the surface of the ^{4}He-rich liquid in the presence of a small, continuous feed of ^{4}He atoms to the vapor phase. This finding is quite surprising since the surface of the ^{4}He-rich phase is covered by an adsorbed layer of ^{3}He atoms which should favor spreading of the ^{3}He-rich liquid.

Owing to the existence of bound states for ^{3}He atoms on the surface of liquid ^{4}He [8], phase separation, below $T_s = 0.87$ K, is expected to nucleate uniformly from a surface layer of ^{3}He. This implies that Antonow's rule for surface tensions is valid, i.e., $\sigma_4 = \sigma_3 + \sigma_{34}$, where σ_3, σ_4, and σ_{34} refer to the ^{3}He-rich phase, the ^{4}He-rich phase, and the phase-separation interface, respectively. Complete wetting of the lower ^{4}He-rich phase by the upper ^{3}He-rich phase would then take place and the contact angle would be zero. Our experimental results demonstrate, however, that the validity of Antonow's rule is destroyed if the vapor phase is kept slightly out of equilibrium. A pool of ^{3}He was formed with a contact angle on the order of 10 mrad.

In our investigations we have employed two-beam optical interferometry [7,9]. The experimental chamber was a copper cylinder ($\phi = 13$ mm, height = 8 mm) with the upper end sealed by a fused silica window whose normal is tilted by 2° off the cylinder axis. The lower end was closed by an antireflection-coated fused silica wedge acting as our optical reference flat. Temperature was measured using a bismuth ruthenate resistor (1 kΩ, Dale Electronics, Norfolk, Nebraska), located on the mixing chamber of our Oxford 600 dilution unit. The $R(T)$ curve of the resistor was calibrated against the phase-separation temperature $T_s = 0.328$ K of the bulk 13.5% ^{3}He/^{4}He mixture [10] by observing the nucleation of ^{3}He-rich liquid in an almost filled chamber when the border of a free surface was visible against the top window. This was considered sufficient since the measurements span only over temperatures $T = 0.25$–0.55 K. A full account of the experimental details will be published elsewhere [11].

In the course of our experiments three different fill lines, made of 0.1-mm CuNi capillaries, were used in separate cool-downs. Two of them ($L = 1$ and 4 m) were well heat sunk into the 1-K plate but only weakly attached to the mixing chamber of our dilution refrigerator. Such a capillary, when not completely full, produces a small continuous recondensation flux of ^{4}He atoms to the experimental cell [12], caused by the flow of a superfluid ^{4}He film along the capillary towards high-temperature regions where the film evaporates. With the third fill line the thermalization at the mixing chamber was improved by a sintered silver heat exchanger which eliminated the recondensation flux of ^{4}He gas to the experimental cell.

Nominal ^{3}He concentrations of 12%–20% were employed. In the experimental space the concentration of ^{3}He was higher than the nominal value since some ^{4}He resided in the fill capillary: partly as an up-climbing superfluid film and partially as down-flowing gas. The actual ^{3}He concentration c_3 in the experimental volume was deduced from the phase-separation temperature of the film, overlooking a small uncertainty caused by our inability to observe phase separation close to the walls. The estimated accuracy of the measured concentrations is 1 unit of percentage.

The thickness of the films was determined by counting the number of interference fringes. In order to speed up relaxation, we worked with films as thick as possible. However, the thickness could not be increased very much because the liquid surface started to vibrate when the depth approached 50 μm. After admitting liquid to

0031-9007/94/73(10)/1388(4)$06.00

the experimental chamber, the interference fringes varied initially with time, probably because the flux of ^{4}He atoms was influenced by some ^{3}He-rich liquid flowing down slowly along the fill capillary. Waiting for more than 24 h ascertained reproducible results: We believe that this time was sufficient for all the ^{3}He to reach the cell.

Our cooled charged coupled device imager [11] required a light power of 100 μW for optimum contrast. About 0.5% of the light was absorbed by the fused silica reference flat and by the top window of the sample cell, which means a heat leak of 0.5 μW caused by the illumination. As in the experiments on superfluid ^{3}He [7], continuous light produced a clear fountain effect in thin superfluid films. Typically, we employed 50 ms light pulses at a rate of 0.1 Hz, which resulted in an average heat leak of 2 nW, well below the thermal load caused by the condensation of ^{4}He atoms from the vapor phase.

The rate at which ^{4}He atoms entered the cell was estimated by inspecting the fountain effect produced by laser illumination: When thermal load from the condensation of ^{4}He atoms onto the film exceeded the heating from light, no fountain effect was observed. So we determined the thermal load caused by ^{4}He atoms from the brightness of the laser beam at which we started to observe the fountain effect. This yielded condensation rates of 5×10^{15} and 10^{15} atoms/cm^2 s for the 1- and 4-m-long fill capillaries, respectively, roughly inversely proportional to the tube length.

Figure 1(a) displays an interferogram of a horizontal liquid surface measured in a $c_3 = 13\%$ ^{3}He/^{4}He mixture at $T = 0.32$ K, above the phase-separation temperature. The pattern of about 40 evenly space straight fringes is caused by a deliberate 0.12° misalignment of the reference flat with respect to the horizon, as illustrated in the inset. This configuration is useful in the analysis of the interferograms, but it also means that the liquid layers under investigation are wedge shaped and their thickness varies by 17 μm over the 9-mm-diam visible area (0.307 μm/fringe).

The patterns in Figs. 1(b) and 1(c) display interferograms measured at $T < T_s$; the separation of the mixture into the ^{3}He- and ^{4}He-rich phases in our experimental cell is schematically illustrated in the inset of Fig. 1(c). The stripelike ^{3}He pattern [(c)] was more stable than the droplet-shaped configuration [(b)], especially in experiments with a large c_3. The structures in Fig. 1(c) were unchanged during several hours at constant temperature whereas slight modifications in the shape of the droplets occurred. Sizes of the pools illustrated in Figs. 1(b) and 1(c) depended strongly on c and T, i.e., on the amount of phase-separated ^{3}He-rich liquid. At $T \ll T_s$, the ^{3}He-rich layer covered the whole visible area and the interferogram displayed a set of straight fringes, similar to the patterning Fig. 1(a).

Creation of the ^{3}He pool took place in the vicinity of walls; i.e., the coldest regions were favored. When the ^{3}He pools entered the field of view they were typically singly connected, stripelike patterns whose width was about 2 mm. Rapid cooling tended to create highly nonuniform, even doubly connected patterns which subsequently relaxed gradually with time and occasionally transformed into almost circular droplets in about 15 min with slow further cooling. Hence, it appears that the generation of droplet-shaped pools was strongly connected with thermal gradients present in the sample during phase separation. At high ^{3}He concentrations, no lens-shaped droplets could be generated. Unfortunately, detailed studies on the formation of pools were limited by the fact that we saw only about 40% of the cross-sectional area of the cylinder.

The level of the ^{4}He-rich phase was horizontal except for a small downturn before the droplet edge [see Fig. 1(b)]. The amount of this downturn varied: The thinner the liquid layer the more the ^{4}He surface bent down before the edge. In films a few microns thick, grooves

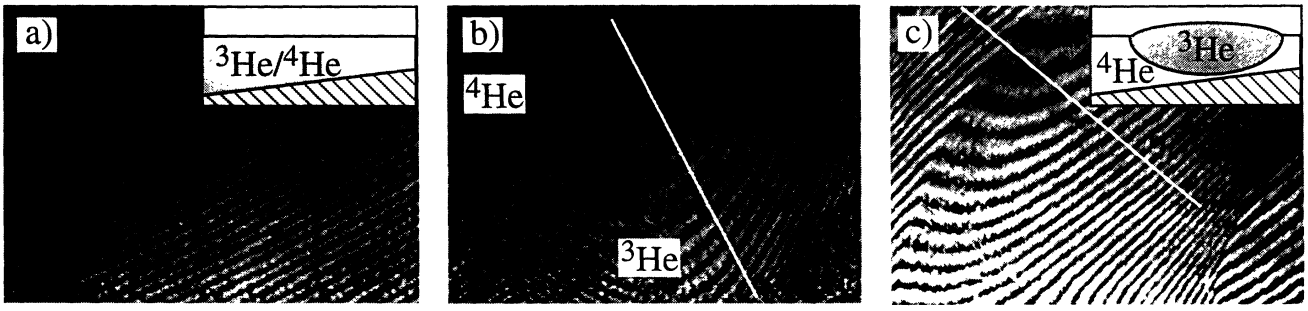

FIG. 1. Interferograms (viewed from above) measured in helium mixture films: (a) $T = 0.32$ K at the ^{3}He concentration $c_3 = 13\%$; (b) $T = 0.30$ K at $c_3 = 13\%$; and (c) $T = 0.32$ K at $c_3 = 15\%$; the displayed area covers 6×8 mm^2. Each fringe denotes an equal depth contour (multiples of 0.307 μm) with respect to the 0.12°-tilted reference plate; the depth of the liquid is largest in the upper left corner. The uniform fringe pattern in Fig. 1(a) corresponds to a wedge-shaped liquid layer, shown schematically in the inset (viewed from the side and the vertical scale magnified by 10^2). The up-bulging region seen in the interferograms (b) and (c) is identified as floating ^{3}He-rich liquid on top of the ^{4}He-rich superfluid as illustrated in the inset of (c). The free surface of the ^{4}He-rich phase is virtually flat, except for a small downturn before the droplet edge [see the upper right corner in (b)]. The overlaid white lines, 4.7 mm long in reality, mark the axes along which we have constructed the surface profiles illustrated in Fig. 2.

exceeding 1 μm were observed next to the edge on the ^{4}He side. Owing to this effect and to various complicated relaxation phenomena observable in thin films, all our results with $d < 20$ μm have been excluded from the present Letter and they will be discussed more fully in a separate publication [11].

Surface contours, obtained by analyzing the interferograms in Figs. 1(b) and 1(c), are displayed in Fig. 2. The profiles were deduced from changes in fringe positions when compared with the flat, horizontal liquid surface in Fig 1(a). For both ^{3}He pools we observe a clear kink in the surface profile which yields an inclination angle $\theta_3 \approx 1.7$ mrad for the ^{3}He surface with respect to the horizon at the edge of the pool. The inclination angle changes somewhat along the droplet border, from 2.5 mrad at left to 1.6 mrad at right. This variation is to be expected since the shape of the droplet is asymmetric as can be seen from the interference fringes. The asymmetry relaxed slowly and no substantial change in the inclination angle could be observed after 1 h. In stripe-shaped pools, the variation of θ_3 was smaller.

Typically, we allowed 1 h for relaxation at constant T. This guaranteed that films down to about $d = 5$ μm were able to relax to the equilibrium shape by viscous flow. In mixtures, however, the relaxation process should speed up by exchange of ^{3}He across the interface to the superfluid phase where mass diffusion is fast owing to second sound [13]. In films with $d > 20$ μm, no dependence of the inclination angle on the depth of the liquid was observed.

The fact that abrupt changes in the interference pattern were created by an edge between the ^{3}He- and ^{4}He-rich phases was verified by applying continuous illumination to the sample, close to T_s. This increased the temperature of the liquid so that the ^{3}He layer vanished gradually by dissolving into the ^{4}He-rich phase. Simultaneously, a set of weak interference rings, whose size shrank with the ^{3}He pool, were resolved: These could be assigned to interference created by reflections from the phase-separation interface and from the reference flat.

Benefiting from the small inclination of the ^{3}He pool edge at $T = 0.51$ K, we succeeded in imaging the free surface and the phase-separation interface simultaneously, which is illustrated in Fig. 3. The interferogram was obtained by subtracting two video frames 80 ms apart in time, recorded during continuous illumination. The interference pattern has two sets of fringes which were investigated separately using self-made polynomial surface fitting extensions to a commercial graphics program (IPLAB, Signal Analytics, Vienna, Virginia). The analysis yields $\theta_3 = 0.8$ mrad and $\theta_{34} = 4.8$ mrad, which makes for the total contact angle $\theta = \theta_3 + \theta_{34} \approx 6$ mrad; this is close to the maximum angle that can be measured by our interferometric method. The ratio $\theta_{34}/\theta_3 = 6$ is too small when compared with the vertical force ratio $\sigma_3/\sigma_{34} = 15$, measured in a $c_3 = 22\%$ mixture at $T = 0.52$ K [14]. The difference may be caused by heat currents in our sample.

No stable pools of ^{3}He were observed in the experimental setup with a sintered silver heat exchanger in the fill line. We were able to create regions of ^{3}He accumulation on the surface by adding more ^{3}He/^{4}He mixture to the experimental volume. However, these pools vanished with a time constant of 10 min and ^{3}He spread evenly over the liquid surface. Therefore, our results do not violate the general view of phase separation under equilibrium

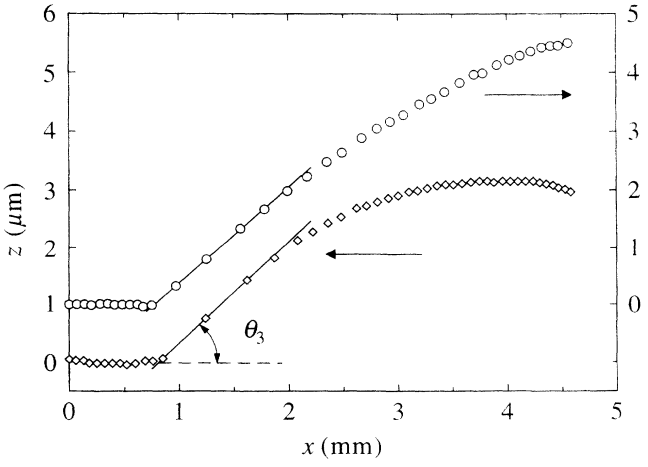

FIG. 2. Contour (viewed from the side) of the liquid surface vs distance x measured from the left end of the 4.7-mm-long lines marked in Figs. 1(b) (○) and 1(c) (◇); both dark and bright fringes were employed in the analysis. Least-squares-fitted straight lines in the region 0.8 mm $< x <$ 1.8 mm yield for the inclination angle $\theta_3 = 1.68$ mrad (○) and 1.78 mrad (◇), respectively. Note the different vertical and horizontal scales.

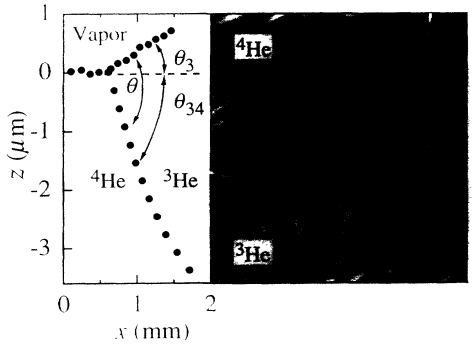

FIG. 3. Profile (viewed from the side) of the ^{3}He-rich liquid bound by the vapor phase and by the ^{4}He-rich superfluid, deduced from the interferogram (viewed from above) at right ($T = 0.51$ K and $c_3 = 24\%$); the x axis spans over the white bar in the fringe pattern, starting from the left end. The dashed line in the interferogram denotes the contact angle θ into the picture, as well as the inclination angles θ_3 and θ_{34} of the ^{3}He-rich surface and of the ^{3}He/^{4}He interface, respectively.

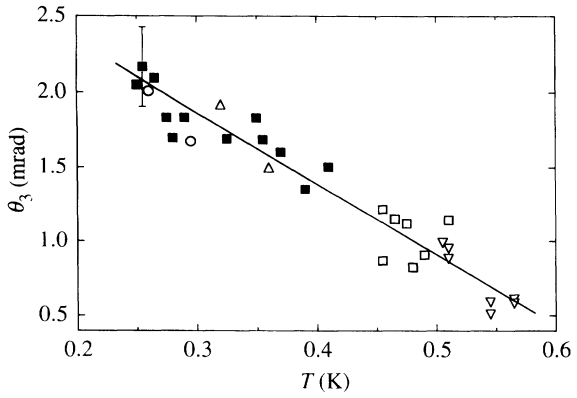

FIG. 4. Inclination angle θ_3 of the liquid surface at the border of the ^{3}He-rich pool vs temperature measured in mixtures with different nominal ^{3}He concentrations: $c_3 = 13\%$ (△, ○), 15% (■), 21% (□), and 24% (▽). The filled and open symbols refer to the 1 and 4-m-long fill capillaries, respectively. The circles denote data on dropletlike pools.

conditions, according to which the trapped layer of ^{3}He atoms on the surface of ^{4}He acts as nucleation center for the ^{3}He-rich upper phase and the contact angle is zero.

Figure 4 summarizes our results on the inclination angle θ_3 as a function of temperature. No clear difference between the points measured using the short (1 m) or the long (4 m) filling capillary is observed. The common tendency in the data is that θ_3 decreases with increasing temperature and seems to approach zero gradually around 0.7 K. This is to be expected since the influence of the reentering ^{4}He gas ought to decrease as the vapor pressure of ^{4}He increases with temperature. At $T = 0.4$ K, the saturated ^{4}He vapor pressure $p = 10^{-5}$ mbar corresponds to roughly 10^{15} atoms in the vapor phase of our experimental cell. Therefore, the incoming ^{4}He flux of $\sim 10^{15}$ atoms/s has its biggest effect below 0.4 K where the gas flow strongly modifies the ^{4}He pressure.

We believe that the finite contact angle observed in our experiments is due to a modification of the ^{3}He surface tension by the condensing ^{4}He atoms. This explanation is based on the large difference in the mass diffusion constants between the superfluid and normal phases [13]: In the former the second sound makes the effective diffusion constant infinite while in normal ^{3}He it remains small. By employing the formula [15] $1 - \cos\theta = [(\sigma_3 - \sigma_{34})^2 - \sigma_4^2]/2\sigma_3\sigma_{34}$, we find that σ_3 has to be increased only by a relative change of 10^{-5} in order to explain our results. A finite contact angle could also be caused by a reduction in σ_4. We think this is unlikely, since σ_4 should grow with increasing ^{4}He concentration [16].

Another possibility is that there is a small temperature drop $\Delta T = T_3 - T_4$ across the interface owing to the Kapitza resistance between the ^{3}He- and ^{4}He-rich phases. Since $d\sigma_3/dT > 0$ [14], a finite contact angle is produced by recondensation ($\Delta T > 0$). Even though the numerical estimates for θ by the acoustic mismatch theory produce reasonable results, it is difficult to explain why the inclination angle is independent of the length of the fill capillary, i.e., of the flux of the recondensing ^{4}He atoms.

In summary, we have obtained by optical interferometry results which show that unexpected wetting problems occur in phase-separated ^{3}He/^{4}He mixtures when the vapor pressure of ^{4}He is maintained above its very low saturation level by a continuous feed of ^{4}He atoms to the vapor space. The inclination angle $\theta_3 = \theta_{34}/[\sigma_3 + \sigma_{34}]$ of the ^{3}He-rich pools was found to decrease strongly with temperature (see Fig. 4) and to extrapolate to zero around 0.7 K.

Useful discussions with T. Ala-Nissilä, S. Balibar, P. Leiderer, O. V. Lounasmaa, A. Parshin, and G. R. Pickett are gratefully acknowledged. This work was financially supported by the Academy of Finland.

[1] P. J. Nacher and J. Dupont-Roc, Phys. Rev. Lett. **67**, 2966 (1991).
[2] E. Cheng, M. W. Cole, W. Saam, and J. Treiner, Phys. Rev. Lett. **67**, 1007 (1991).
[3] K. S. Ketola, S. Wang, and R. B. Hallock, Phys. Rev. Lett. **68**, 201 (1992); S. K. Mukherjee, D. P. Druist, and M. H. W. Chan, J. Low Temp. Phys. **87**, 113 (1992); P. Taborek and J. E. Rutledge, Phys. Rev. Lett. **68**, 2184 (1992); J. E. Rutledge and P. Taborek, Phys. Rev. Lett. **69**, 937 (1992).
[4] M. S. Petterson and W. F. Saam, J. Low Temp. Phys. **90**, 159 (1993).
[5] K. S. Ketola and R. B. Hallock, Phys. Rev. Lett. **71**, 3295 (1993).
[6] J. Treiner, E. Cheng, M. Cole, and W. Saam, J. Low Temp. Phys. (to be published).
[7] A. J. Manninen, J. P. Pekola, G. M. Kira, J. P. Ruutu, A. V. Babkin, H. Alles, and O. V. Lounasmaa, Phys. Rev. Lett. **69**, 2392 (1992).
[8] A. F. Andreev, Zh. Eksp. Teor. Fiz. **50**, 1415 (1966) [Sov. Phys. JETP **23**, 939 (1966)].
[9] P. L. Marston and W. M. Fairbank, Phys. Rev. Lett. **39**, 1208 (1977); P. L. Marston, Ph.D. thesis, Stanford University, 1976.
[10] J. Wilks and D. S. Betts, *Introduction to Liquid Helium* (Clarendon, Oxford, 1987), 2nd ed., p. 106, and references therein.
[11] H. Alles, J. P. Ruutu, A. V. Babkin, and P. J. Hakonen, (to be published).
[12] O. E. Vilches and J. C. Wheatley, Rev. Sci. Instrum. **37**, 819 (1966).
[13] G. Ahlers and F. Pobell, Phys. Rev. Lett. **32**, 144 (1974).
[14] H. M. Guo, D. O. Edwards, R. E. Sarwinski, and J. T. Tough, Phys. Rev. Lett. **27**, 1259 (1971).
[15] See, e.g., J. S. Rowlinson and B. Widom, *Molecular Theory of Capillarity* (Clarendon, Oxford, 1982), p. 211.
[16] See, e.g., D. O. Edwards and W. F. Saam, in *Progress in Low Temperature Physics VIIA*, edited by D. F. Brewer (North-Holland, Amsterdam, 1978), p. 297.

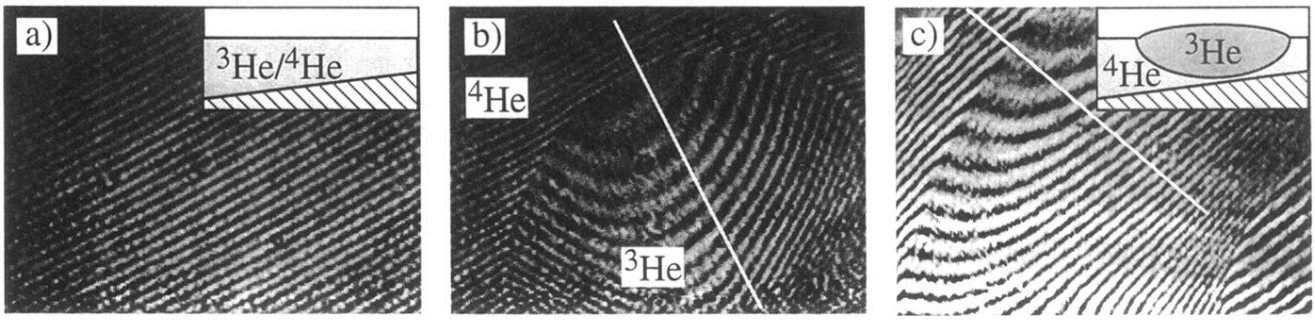

FIG. 1. Interferograms (viewed from above) measured in helium mixture films: (a) $T = 0.32$ K at the ^{3}He concentration $c_3 = 13\%$; (b) $T = 0.30$ K at $c_3 = 13\%$; and (c) $T = 0.32$ K at $c_3 = 15\%$; the displayed area covers 6×8 mm^2. Each fringe denotes an equal depth contour (multiples of 0.307 μm) with respect to the 0.12°-tilted reference plate; the depth of the liquid is largest in the upper left corner. The uniform fringe pattern in Fig. 1(a) corresponds to a wedge-shaped liquid layer, shown schematically in the inset (viewed from the side and the vertical scale magnified by 10^2). The up-bulging region seen in the interferograms (b) and (c) is identified as floating ^{3}He-rich liquid on top of the ^{4}He-rich superfluid as illustrated in the inset of (c). The free surface of the ^{4}He-rich phase is virtually flat, except for a small downturn before the droplet edge [see the upper right corner in (b)]. The overlaid white lines, 4.7 mm long in reality, mark the axes along which we have constructed the surface profiles illustrated in Fig. 2.

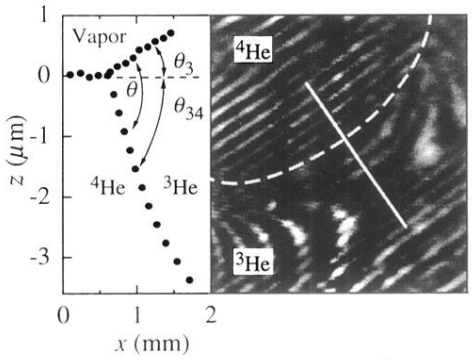

FIG. 3. Profile (viewed from the side) of the ^{3}He-rich liquid bound by the vapor phase and by the ^{4}He-rich superfluid, deduced from the interferogram (viewed from above) at right ($T = 0.51$ K and $c_3 = 24\%$); the x axis spans over the white bar in the fringe pattern, starting from the left end. The dashed line in the interferogram denotes the contact angle θ into the picture, as well as the inclination angles θ_3 and θ_{34} of the ^{3}He-rich surface and of the ^{3}He/^{4}He interface, respectively.